Joint Centre for Mesoscale Meteorology, Reading, UK

Potential Vorticity Inversion

M. Ziemianski

Internal Report No. 39

October 1994

Met Office Joint Centre for Mesoscale Meteorology Department of Meteorology
University of Reading PO Box 243 Reading RG6 6BB United Kingdom
Tel: +44 (0)118 931 8425 Fax: +44 (0)118 931 8791
www.metoffice.com

Designed and produced by the Met Office © Crown copyright 2001 01/0240 The Met Office logo is a registered trademark.

Potential Vorticity Inversion

Michal Ziemianski
Institute of Meteorology and Water Management
Maritime Branch
Gdynia Weather Office
Poland

Report on work performed under the Meteorological Office Visiting Scientist Programme at the Joint Centre for Mesoscale Meteorology Meteorological Office/University of Reading

Reading, October 1994

1. Summary.

A program for inverting Ertel's potential vorticity was accomplished. It was used to calculate flow and temperature fields induced by idealised potential vorticity distribution and by potential vorticity in real atmosphere. The routine was used also for attributing flow patterns induced by individual potential vorticity anomalies during cyclogenesis event over North-Eastern Atlantic and Europe between 12 and 14 January 1993.

2. Introduction.

In theoretical and operational meteorology there is a need for an appropriate tool for diagnosing dynamical aspects of cyclogenesis events. The tool should be possibly simple but rooted in basic physical principles governing atmospheric flow. It should allow to develop simple and adequate conceptual model or models of these processes which would increase our understanding and help in improving weather forecasts through better diagnostics of current weather and better assessment of the quality of current output from operational prognostic models.

The Ertel's potential vorticity, defined as

$$q = \frac{1}{\rho}\vec{\eta}\cdot\vec{\nabla}\theta$$

where ρ -density, $\vec{\eta}$ -absolute vorticity vector and θ -potential temperature (Rossby 1940, Ertel 1942), seems to be a good candidate for such a tool.

It is a simple scalar quantity conserved following adiabatic and frictionless motion. If, additionally, a relation between the wind and temperature (or mass) distribution is provided (balance equation) it allows calculating of the wind and mass distribution for specified boundary conditions by inverting an elliptic differential equation for q (Hoskins, McIntyre and Robertson 1985).

The special value of potential vorticity in diagnosing atmospheric flows was confirmed by its crucial role in theory of baroclinic instability (Charney, Stern 1962).

3. Method.

During realization of this program the work of Christopher Da-

vis and Kerry Emanuel (1991) was followed. The potential vorticity inverter was constructed as follows:

Starting from the potential vorticity equation in pressure coordinates

$$q = -g\vec{\eta}\cdot\vec{\nabla}\theta$$

and dropping components of the vorticity vector connected with vertical velocity we obtain

$$q = -g\left[\left(\frac{\partial v}{\partial x} - \frac{\partial u}{\partial y} + f\right)\frac{\partial\theta}{\partial p} - \frac{\partial v}{\partial p}\frac{\partial\theta}{\partial x} + \frac{\partial u}{\partial p}\frac{\partial\theta}{\partial y}\right]$$

where u - x-component and v - y-component of wind velocity, f - Coriolis parameter.

Following scale analysis we can assess that the divergent part of wind velocity is roughly an order of magnitude less than its rotational part. Therefore only the nondivergent part of wind is retained, which gives

$$\vec{v} = \vec{k}\times\vec{\nabla}\psi$$

$$q = -g\left[\left(f + \nabla^2\psi\right)\frac{\partial\theta}{\partial p} - \frac{\partial^2\psi}{\partial x\partial p}\frac{\partial\theta}{\partial x} - \frac{\partial^2\psi}{\partial y\partial p}\frac{\partial\theta}{\partial y}\right]$$

where $\vec{v}$ - wind welocity, $\vec{k}$ - unit vertical vector, ψ - stream function.

Introducing the Exner vertical coordinate

$$\pi(p) = c_p\left(p/p_0\right)^{\varkappa}$$

where $\varkappa = R/c_p$ and using the hydrostatic equation in this coordinate frame

$$\frac{\partial\phi}{\partial\pi} = -\theta$$

where ϕ - geopotential, we obtain finally the potential vorticity equation in form:

$$q = \frac{g\varkappa\pi}{p}\left[\left(f + \nabla^2\psi\right)\frac{\partial^2\phi}{\partial\pi^2} - \frac{\partial^2\psi}{\partial x\partial\pi}\frac{\partial^2\phi}{\partial x\partial\pi} - \frac{\partial^2\psi}{\partial y\partial\pi}\frac{\partial^2\phi}{\partial y\partial\pi}\right] \qquad (*)$$

The second equation is Charney's nonlinear balance equation (Charney 1955)

$$\nabla^2\phi = \vec{\nabla}\left(f\cdot\vec{\nabla}\psi\right) + 2\left[\frac{\partial^2\psi}{\partial x^2}\frac{\partial^2\psi}{\partial y^2} - \left(\frac{\partial^2\psi}{\partial x\partial y}\right)^2\right] \qquad (**)$$

The inversion of Ertel's potential vorticity means solving these two equations for ϕ and ψ. It is performed using an iterative method. In practice the sum and difference of (*) and (**) equations are solved which gives a 3-dimensional elliptic Poisson-like equation for ϕ and 2-dimensional elliptic Poisson equation for ψ.

The boundary conditions are Dirichlet condition for ϕ on lateral boundaries (ϕ equals observed geopotential) and Neumann condition on top and bottom of the domain ($\partial\phi/\partial\pi$ equals minus the observed potential temperature). For ψ there is a Dirichlet boundary condition based on normal component of observed wind on

lateral boundaries.

The inversion domain and distribution of grid points match the output of the LAM of the Met Office as used at the Joint Centre for Mesoscale Meteorology in Reading. Horizontally the domain consists of 61 (in x-direction) per 38 (in y-direction) grid points with basic spacing of 108.9 km. Vertically the domain consists of 9 constant pressure levels from 900 to 100 mb with constant spacing of 100 mb.

4. Results.

A. Idealised case.

The routine was used to calculate the wind and potential temperature distribution induced by an idealized potential vorticity anomaly.

The geopotential and stream function were calculated in a domain of 40 by 40 grid points horizontally, 108.9 km apart and bounded by constant pressure surfaces 900 mb on bottom and 200 mb on top. Constant potential temperatures 12°C on the bottom and 62°C on the top were applied. The ambient static stability was presumed constant in the domain. Lateral boundary conditions for ϕ were calculated using the hydrostatic relation and ψ was equal 0 on lateral boundaries.

Finally a potential vorticity anomaly with Gaussian shape in every dimension with characteristic length scale 217.8 km horizontally and 50 mb vertically and maximum 9PVU was inserted in the middle of the domain.

The inversion was performed for 5, 9 and 17 pressure levels equally spaced in the Exner coordinate. Maximum wind velocity, which occurs at the level of the center of anomaly, is a function of the number of levels in the domain and equals: for 5 level inversion 21.0 m/s, for 9 level 17.5 m/s and for 17 level inversion 17.2 m/s.

The distribution of potential vorticity and results of the 9 level inversion are presented in Fig.1 and Fig.2.

The distribution of potential temperature was calculated using the hydrostatic relation so that for calculating potential temperature on coordinate surface values of geopotential on both neighbouring surfaces were used.

B. Real case.

The routine was used also for calculating the balanced rotational wind and potential temperature distribution in real atmosphere.

For performing the inversion the meteorological situation from 00z, 8 August 1994 was chosen. At this time a significant potential vorticity anomaly was penetrated from the stratosphere

to mid tropospheric altitudes over the Eastern Atlantic inducing a cold low down to the sea surface.

The distribution of potential vorticity and boundary conditions were taken from the LAM using MDIAG procedures. Boundary conditions for ϕ were calculated using distribution of potential temperature and hydrostatic relation.

Potential temperature on the coordinate surfaces was calculated using potential temperature on coordinate surface immediately below and the hydrostatic relation between these two surfaces.

Results of the inversion compared with real data are presented on Fig.3 to Fig.8.

Average differences between real wind and inverted wind vary from 35% on bottom to 10% in the middle of the model. The maximum difference equals 10 m/s. The average difference on the top reaching 75% seems to be caused by a model analysis error.

For the other case, from 06z, 13 January 1993, where wind velocities were greater, especially in lower levels, average differences between real and inverted wind vary from 23% on bottom to 10% in the middle of the domain. The maximum difference reaches 13 m/s. The average difference on the top equals 32%.

The results could be regarded as satisfactory, taking into consideration that the real atmospheric flow is not balanced, especially in the boundary layer region, and the routine does not take account of the divergent component of wind velocity.

C. Attribution.

The inversion was used also for an attribution problem, in which routine allows to calculate the part of flow, which is induced by a particular potential vorticity anomaly.

Unfortunately the problem of attribution is ambiguous, which results from the nonlinear form of the potential vorticity and balance equations, difficulties in defining basic state and anomalies for the real atmosphere and ambiguity in prescribing boundary conditions for inversion (Davis 1992, Bishop and Thorpe 1994).

Bearing these difficulties in mind it is possible to perform the calculation and obtain satisfactorily results using possibly acceptable basic assumptions.

Here potential vorticity anomalies were defined in terms of the time averaged basic state. The flow connected with a particular potential vorticity anomaly was calculated as a difference between the wind induced by the full distribution of potential vorticity and a wind obtained by inversion of potential vorticity distribution where this particular anomaly was replaced by the mean, basic state. The boundary conditions for this second inversion were left unchanged.

The results of this attribution are presented on Figs. 9 and 10.

They show very clearly the mutual amplification of the lower anomaly of potential temperature and upper level potential vorticity anomaly in accordance with the general picture of baroclinic instability as a superposition of two mutually amplifying Rossby waves (Hoskins, McIntyre and Robertson 1985).

5. Conclusion.

The results of diagnosing atmospheric flow and dynamics of a real cyclogenesis event using Ertel's form of the potential vorticity and the nonlinear balance equation are encouraging. Especially that they proved to be useful for studying generation of a low of scale smaller than other lows investigated using similar methods before.

Further studies are possible both in using the method for diagnosing other real events, perhaps of even smaller scale (polar lows for instance), and in improving the method itself (by including the balanced divergent part of the wind for instance).

Finally I would like to thank The Meteorological Office for funding my work within the Visiting Scientist Programme and to thank all the members of JCMM for great help and support.

References:

Bishop, C.H. and Thorpe, A.J., 1994: Potential Vorticity and the electrostatic analogy: quasi-geostrophic theory. Quart. J. Roy. Met. Soc.,

Charney, J.G., 1955: The use of primitive equations of motion in numerical prediction. Tellus, 7, 22-26.

Charney, J.G. and Stern, M.E., 1962: On the stability of internal baroclinic jets in rotating atmosphere., J. Atmos. Sci., 19, 159-172.

Davis, Ch.A., 1992: Piecewise potential vorticity inversion., J. Atmos. Sci., 49, 1397-1411.

Davis, Ch.A. and Emanuel K.A., 1991: Potential vorticity diagnostics of cyclogenesis., Mon. Wea. Rev., 119, 1929-1953.

Ertel H., 1942: Ein neuer hydrodynamisher wirbelsatz. Meteor. Z., 59, 271-281.

Hoskins, B.J., McIntyre, M.E., Robertson, A.W., 1985: On the use and significance of isentropic potential vorticity maps., Quart. J. Roy. Met. Soc., 111, 877-946.

Rossby, C.G., 1940: Planetary flow patterns in the atmosphere., Quart. J. Roy. Met. Soc., 66, 68-87.

Figure legends.

Fig.1. Potential vorticity distribution for idealised case with 9 PVU anomaly. Vertical cross-section through PV anomaly maximum (isolines every 1 PVU).

Fig.2. Potental temperature and wind velocity induced by 9 PVU anomaly of potential vorticity. Vertical cross-section like in Fig.1. Wind velocity component normal to the cross-section every 3 m/s, potential temperature every 9 C.

Fig.3. Potential vorticity distribution at 00z, 8. 08. 1994 in the LAM domain. West-east vertical cross-section through the maximum of potential vorticity anomaly (the position of maximum PV anomaly is 43 N, 22 W).

Fig.4. Distribution of wind velocity and potential temperature from the LAM analisis at 00z, 8. 08. 1994. Verical cross -section like in Fig.3. Wind velocity component normal to the cross-section every 5 m/s, potential temperature every 10 C.

Fig.5. Distribution of wind velocity and potential temperature from potential vorticity inversion at 00z, 8. 08. 1994. Definition of cross-section and isolines like in Fig.4.

Fig.6. Potential vorticity distribution at 00z, 8. 08. 1994 in the LAM domain. North-south vertical cross-section through the maximum of potential vorticity anomaly.

Fig.7. Distribution of wind velocity and potential temperature from the LAM analisis at 00z, 8. 08. 1994. Verical cross -section like in Fig.6. Wind velocity component normal to the cross-section every 5 m/s, potential temperature every 10 C.

Fig.8. Distribution of wind velocity and potential temperature from potential vorticity inversion at 00z, 8. 08. 1994. Definition of cross-section and isolines like in Fig.7.

Fig.9. Potential temperature and wind induced by low-level potential vorticity anomaly on tropopause defined as PV = 2 PVU surface (low level potential vorticity anomaly is collocated with potential temperature anomaly on 900 mb surface). Potential temperature every 4 C.

Fig 10. Potential temperature and wind induced by stratospheric and high-tropospheric potential vorticity anomalies on 900 mb surface. Potential temperature every 2 C.

Fig. 1.

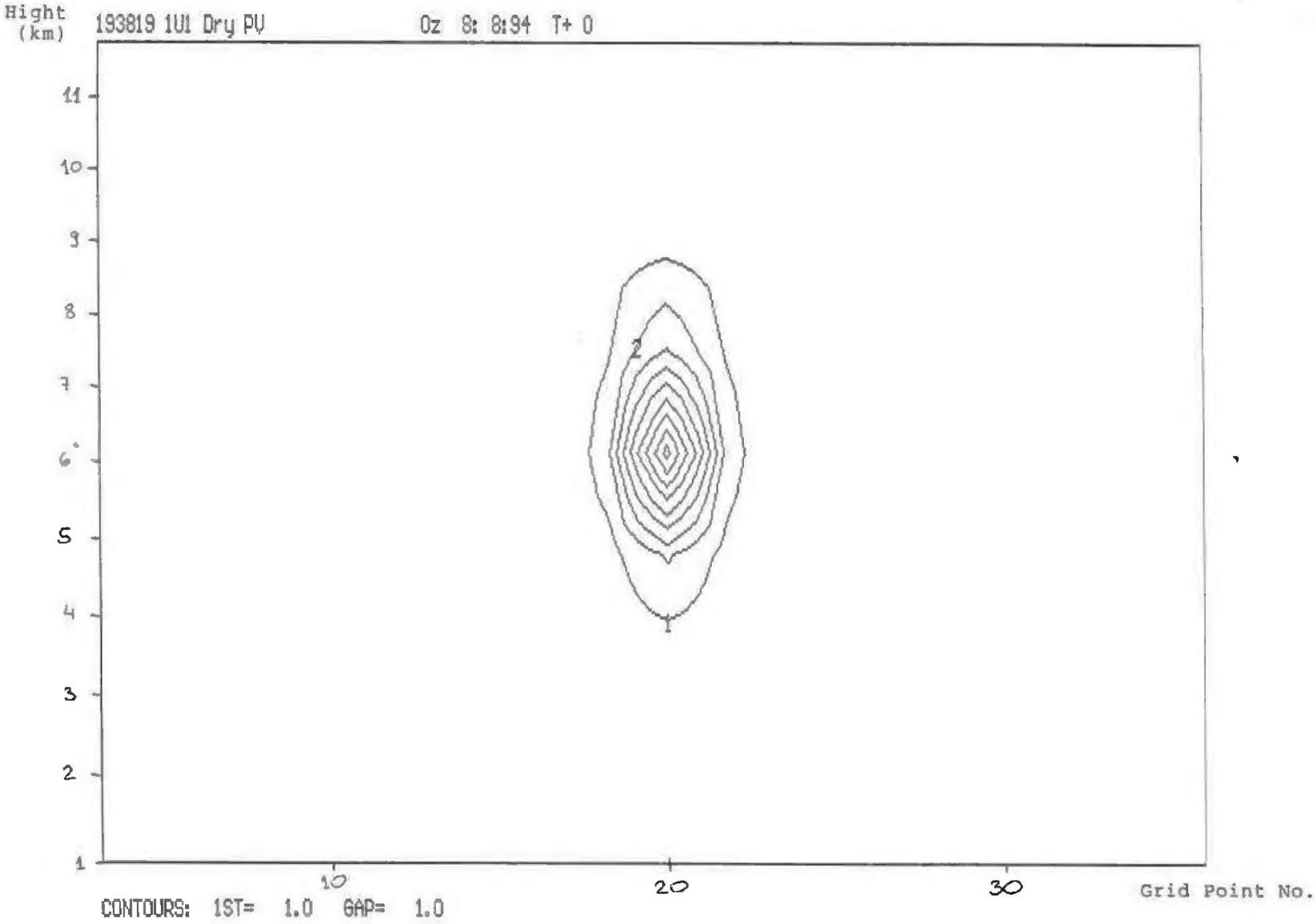
Hight (km)
193819 1U1 Dry PV
Oz 8: 8:94 T+ 0
11
10
9
8
7
6
5
4
3
2
1
2
1
10
20
30
Grid Point No.
CONTOURS: 1ST= 1.0 GAP= 1.0

Fig. 2.

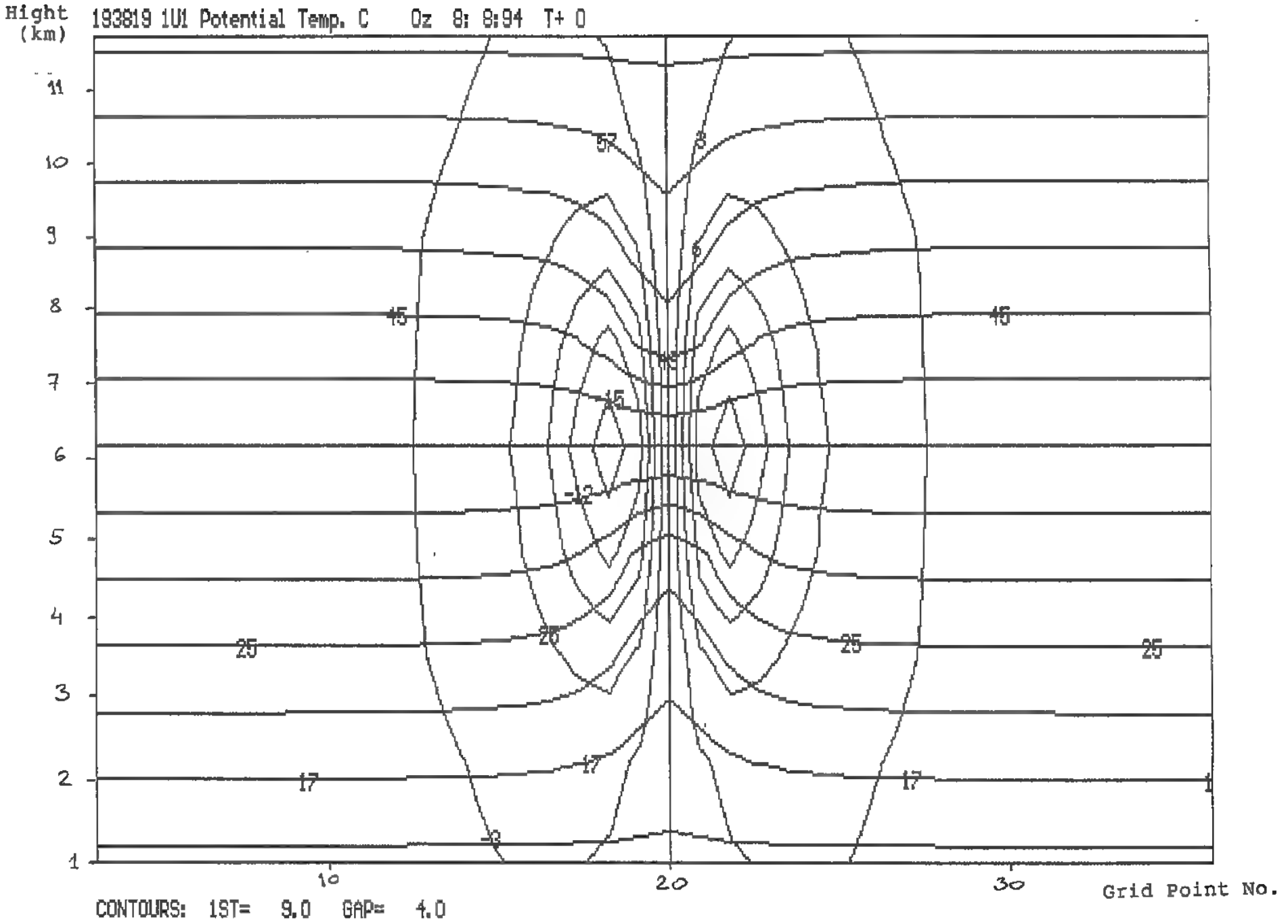

Hight (km)
193819 1U1 Potential Temp. C Oz 8: 8:94 T+ 0
11
10
9
8
7
6
5
4
3
2
1
57
3
6
45
45
45
15
-12
25
25
25
25
17
17
17
-3
10
20
30
Grid Point No.
CONTOURS: 1ST= 9.0 GAP= 4.0

Fig. 3.

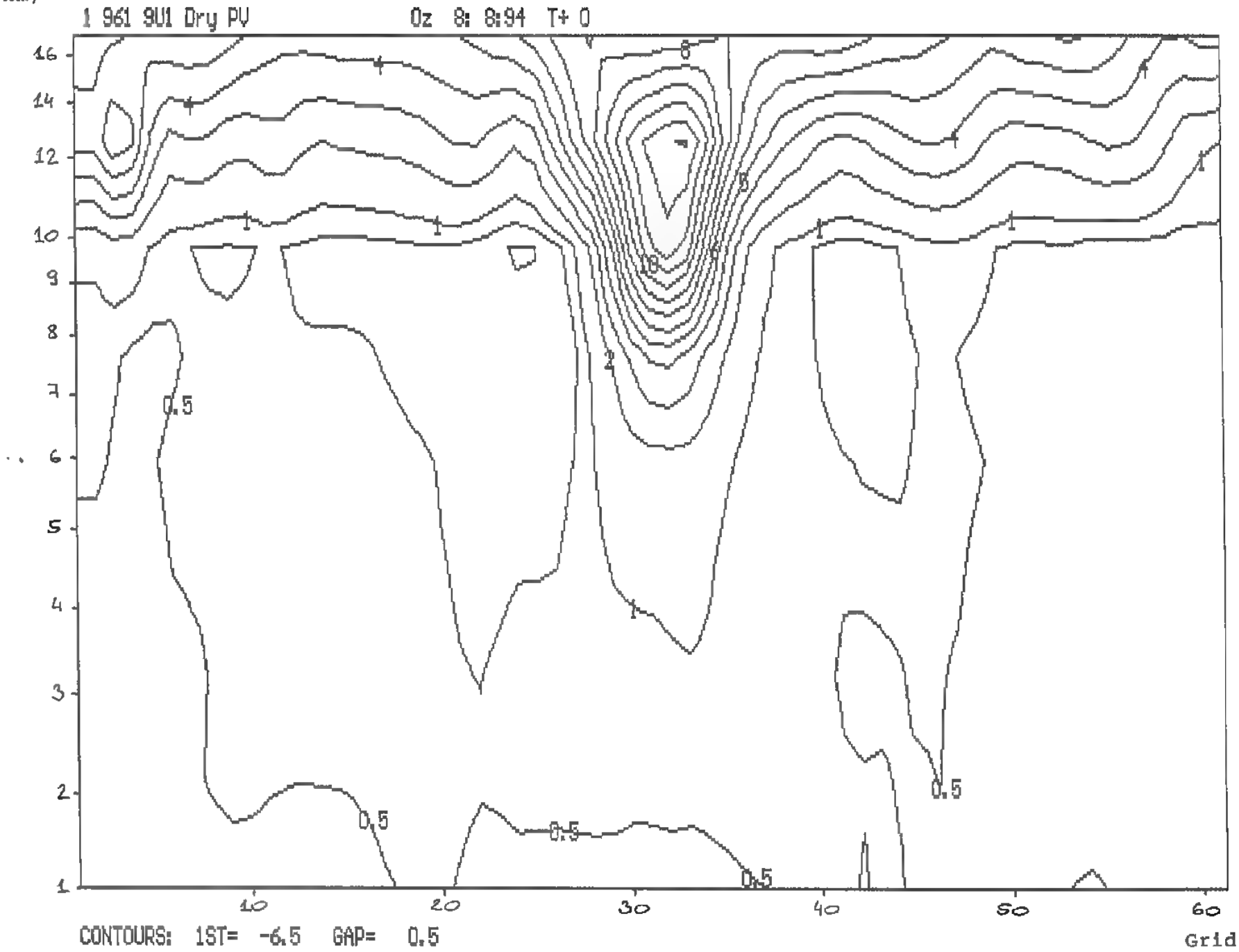
Hight
(km)
1 961 9U1 Dry PV
0z 8: 8:94 T+ 0
16
14
12
10
9
8
7
6
5
4
3
2
1
0.5
0.5
0.5
0.5
0.5
10
20
30
40
50
60
CONTOURS: 1ST= -6.5 GAP= 0.5
Grid Point No.

Fig. 4.

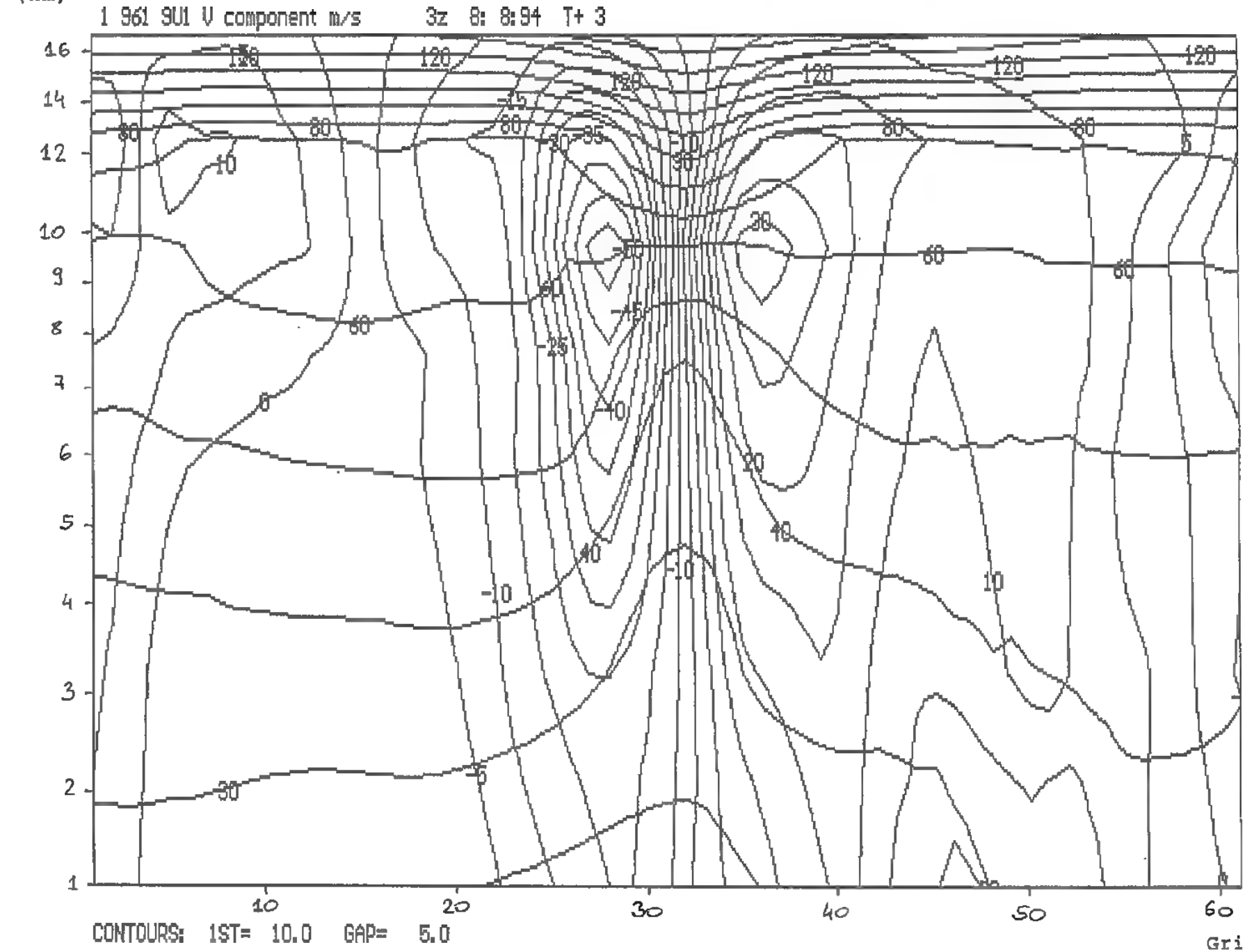
Hight
(km)
1 961 9U1 V component m/s 3z 8: 8:94 T+ 3
16
14
12
10
9
8
7
6
5
4
3
2
1
10
20
30
40
50
60
CONTOURS: 1ST= 10.0 GAP= 5.0
Grid Point No.

Fig. 5.

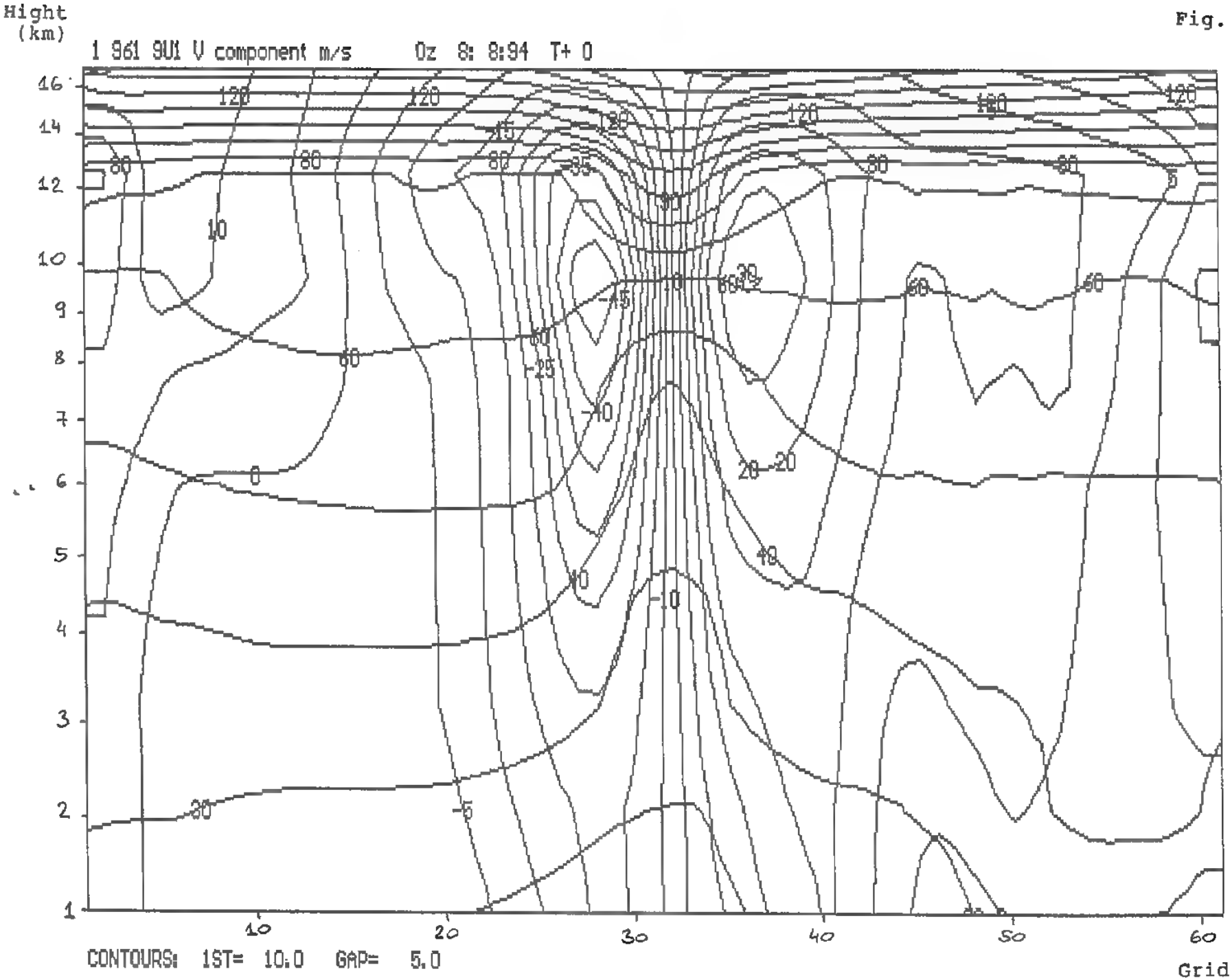
Hight
(km)
1 961 9UI V component m/s
Oz 8: 8:94 T+ 0
16
14
12
10
9
8
7
6
5
4
3
2
1
10
20
30
40
50
60
CONTOURS: 1ST= 10.0 GAP= 5.0
Grid Point No.

Fig. 6.

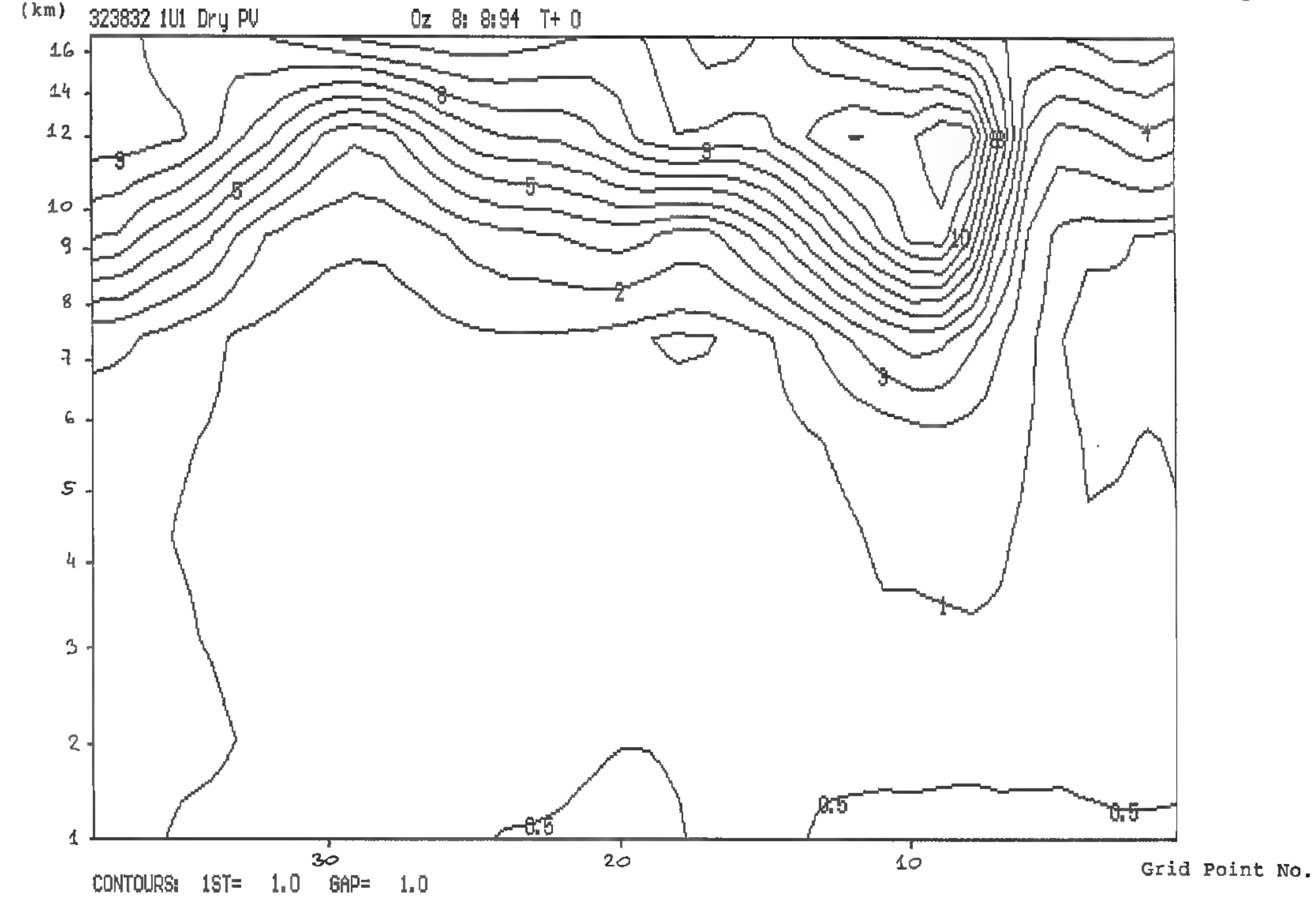
Hight
(km)
323832 IU1 Dry PV
Oz 8: 8:94 T+ 0
16
14
12
10
9
8
7
6
5
4
3
2
1
9
8
7
6
5
4
3
2
1
0.5
0.5
0.5
30
20
10
Grid Point No.
CONTOURS: 1ST= 1.0 GAP= 1.0

Fig. 7.

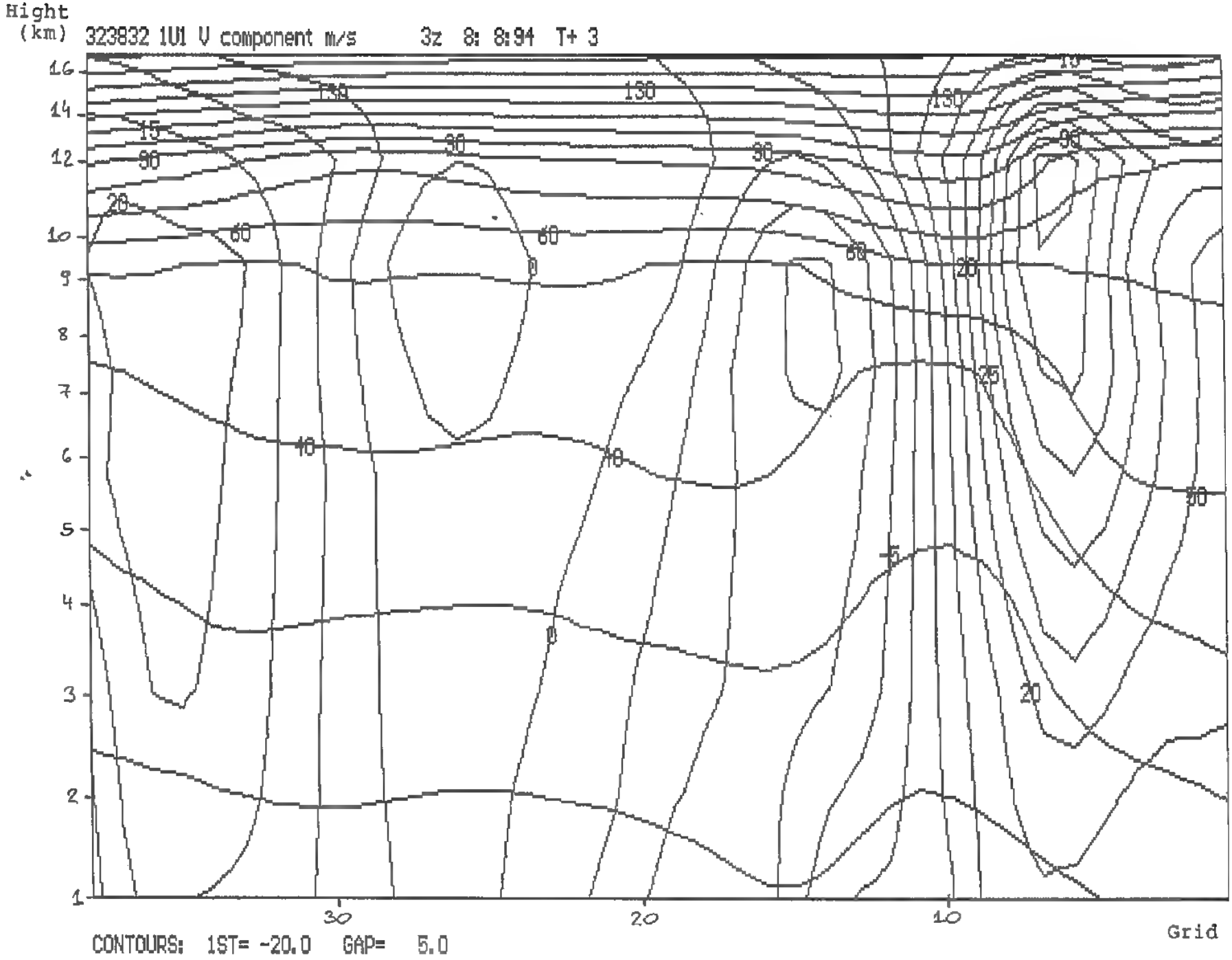
Hight
(km)
323832 1U1 V component m/s
3z 8: 8:94 T+ 3
16
14
12
10
9
8
7
6
5
4
3
2
1
30
20
10
CONTOURS: 1ST= -20.0 GAP= 5.0
Grid Point No.

Fig. 8.

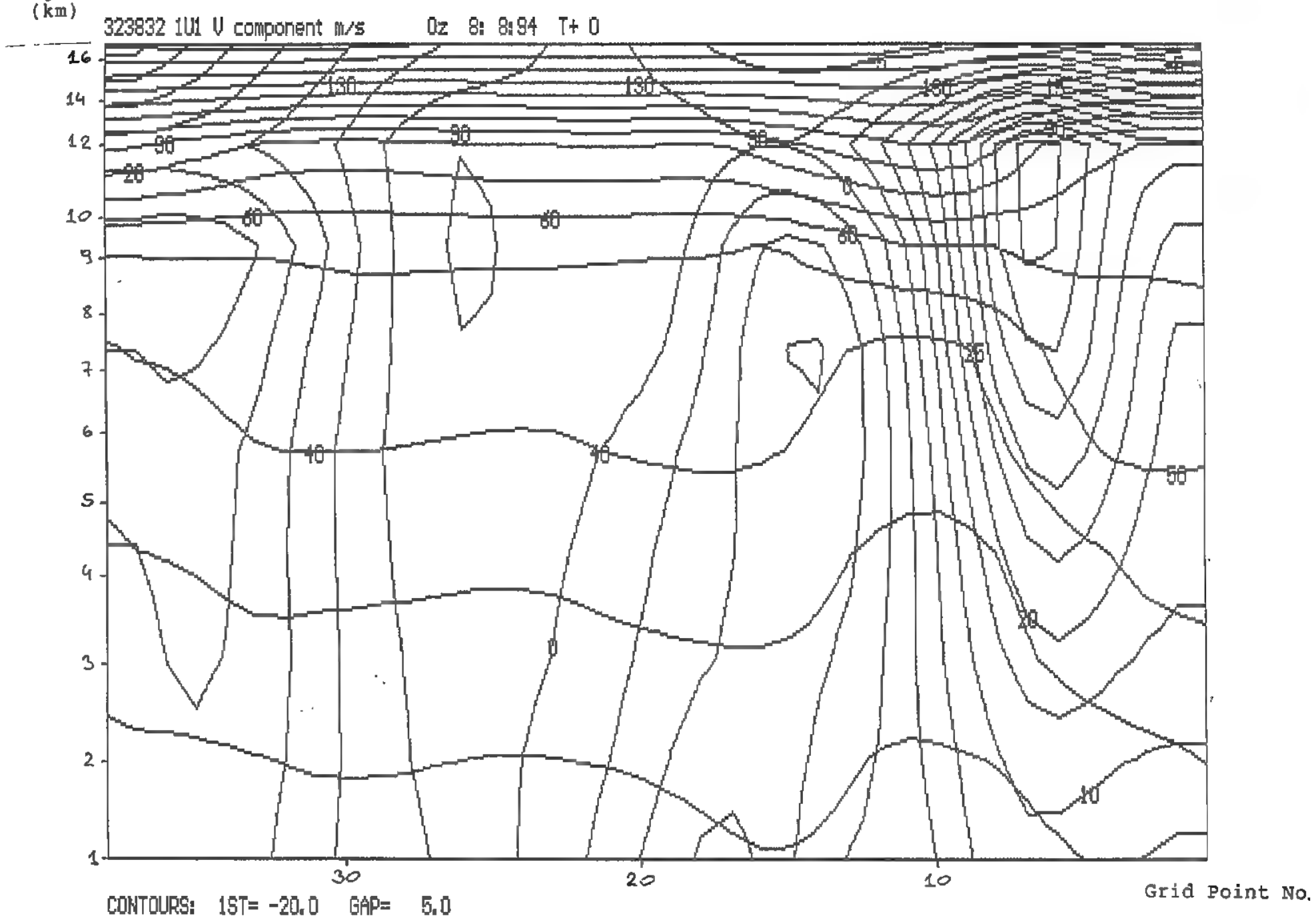
Hight
(km)
323832 1U1 V component m/s
0z 8: 8:94 T+ 0
16
14
12
10
9
8
7
6
5
4
3
2
1
30
20
10
Grid Point No.
CONTOURS: 1ST= -20.0 GAP= 5.0

Fig. 9.

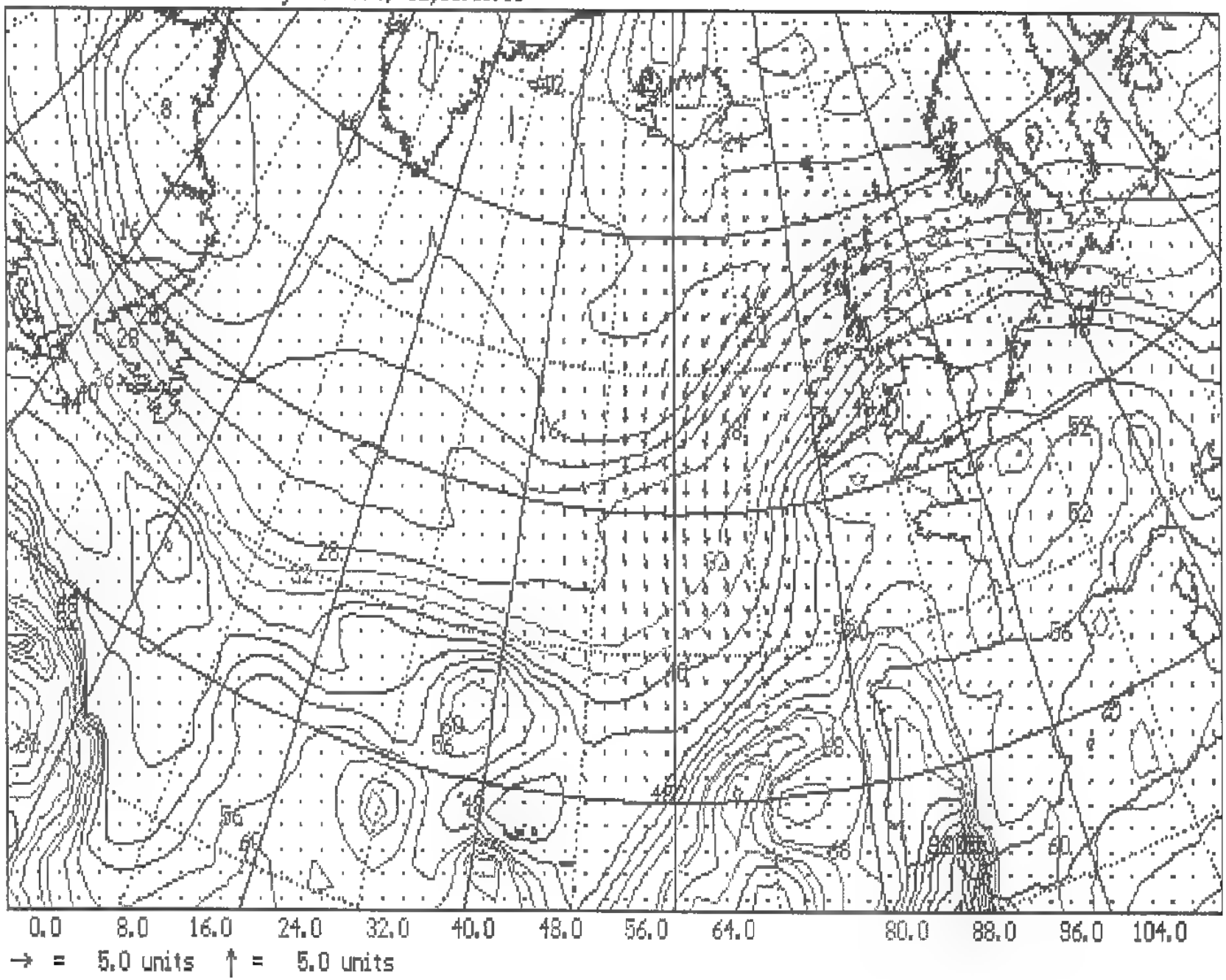
PV=2 Pot.T.+Wind induc. by low-1.PV; 6z,13.01.93
0.0
8.0
16.0
24.0
32.0
40.0
48.0
56.0
64.0
80.0
88.0
96.0
104.0
→ = 5.0 units ↑ = 5.0 units

Fig. 10.

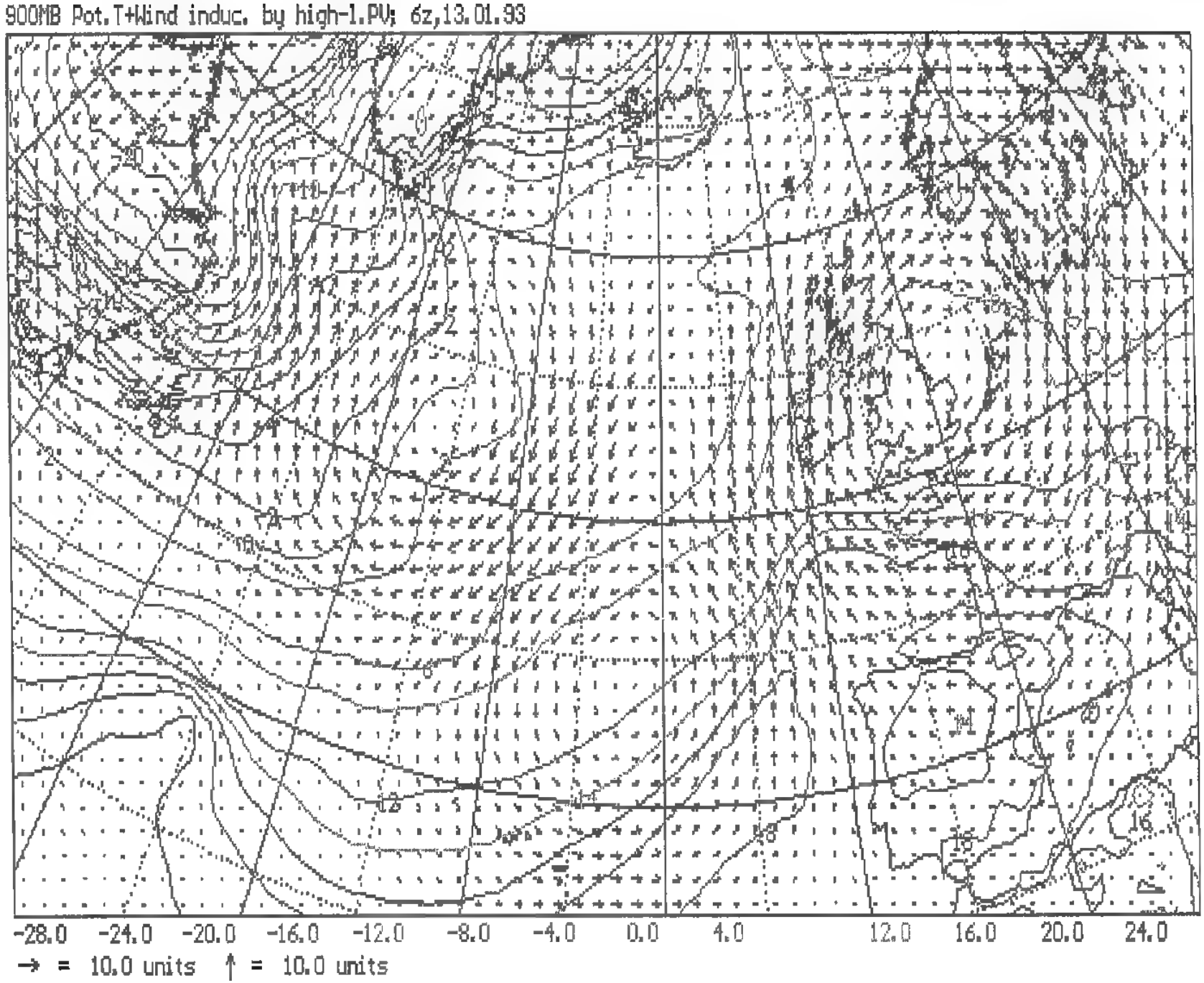
900MB Pot.T+Wind induc. by high-l.PV; 6z,13.01.93
-28.0 -24.0 -20.0 -16.0 -12.0 -8.0 -4.0 0.0 4.0 12.0 16.0 20.0 24.0
→ = 10.0 units ↑ = 10.0 units

CURRENT JCMM INTERNAL REPORTS

This series of JCMM Internal Reports, initiated in 1993, contains unpublished reports and also versions of articles submitted for publication. The complete set of Internal Reports is available from the National Meteorology Library on loan, if required.

1. **Research Strategy and Programme.**
   K A Browning et al
   January 1993

2. **The GEWEX Cloud System Study (GCSS).**
   GEWEX Cloud System Science Team
   January 1993

3. **Evolution of a mesoscale upper tropospheric vorticity maximum and comma cloud from a cloud-free two-dimensional potential vorticity anomaly.**
   K A Browning
   January 1993

4. **The Global Energy and Water Cycle**
   K A Browning
   July 1993

5. **Structure of a midlatitude cyclone before occlusion.**
   K A Browning and N Roberts
   July 1993

6. **Developments in Systems and Tools for Weather Forecasting.**
   K A Browning and G Szejwach
   July 1993

7. **Diagnostic study of a narrow cold frontal rainband and severe winds associated with a stratospheric intrusion.**
   K A Browning and R Reynolds
   August 1993

8. **Survey of perceived priority issues in the parametrizations of cloud-related processes in GCMs.**
   K A Browning
   September 1993

9. **The Effect of Rain on Longwave Radiation.**
   I Dharssi
   September 1993

10. **Cloud Microphysical Processes - A Description of the Parametrization used in the Large Eddy Model.**
H Swann
July 1994

11. **An Appreciation of the Meteorological Research of Ernst Kleinschmidt.**
A J Thorpe
May 1992

12. **Potential Vorticity of Flow Along the Alps.**
A J Thorpe, H Volkert and Dietrich Heimann
August 1992

13. **The Representation of Fronts.**
A J Thorpe
January 1993

14. **A Parametrization Scheme for Symmetric Instability: Tests for an Idealised Flow.**
C S Chan and A J Thorpe
February 1993

15. **The Fronts 92 Experiment: a Quicklook Atlas.**
Edited by T D Hewson
November 1993

16. **Frontal wave stability during moist deformation frontogenesis. Part 1. Linear wave dynamics**
C H Bishop and A J Thorpe
May 1993

17. **Frontal wave stability during moist deformation frontogenesis. Part 2. The suppression of non-linear wave development.**
C H Bishop and A J Thorpe
May 1993

18. **Gravity waves in sheared ducts.**
S Monserrat and A J Thorpe
October 1993

19. **Potential Vorticity and the Electrostatics Analogy: Quasi-Geostrophic Theory.**
C Bishop and A J Thorpe
November 1993

20. **Recent Advances in the Measurement of Precipitation by Radar.**
A J Illingworth
April 1993

21. **Micro-Physique et Givrage. Cloud Microphysics and Aircraft Icing.**
A J Illingworth
May 1993

22. **Differential Phase Measurements of Precipitation.**
M Blackman and A J Illingworth
May 1993

23. **Estimation of Effective Radius of Cloud Particles from the Radar Reflectivity.**
N I Fox and A J Illingworth
May 1993

24. **A Simple Method of Dopplerising a Pulsed Magnetron Radar.**
L Hua, A J Illingworth and J Eastment
November 1993

25. **Radiation and Polar Lows.**
George C Craig
February 1994

26. **Collected preprints submitted to International Symposium on the Life Cycles of Extratropical Cyclones; Bergen, Norway, 27 June - 1 July 1994**
April 1994

27. **Convective Frontogenesis**
Douglas J Parker and Alan J Thorpe
April 1994

28. **Improved Measurement Of The Ice Water Content In Cirrus Using A Total Water Evaporator**
Philip R A Brown and Peter N Francis
April 1994

29. **Mesoscale Effects of a Dry Intrusion within a Vigorous Cyclone**
K A Browning and B W Golding
April 1994

30. **GEWEX Cloud System Study, Science Plan**
May 1994

31. **Parametrization of Momentum Transport by Convectively Generated Gravity Waves**
R Kershaw
May 1994

32. **Mesoscale Modelling Newsletter, No. 5**
May 1994

33. **Observations of the mesoscale sub-structure in the cold air of a developing frontal cyclone**
K A Browning, S A Clough, C S A Davitt, N M Roberts and T D Hewson
May 1994

34. **Longwave Radiative Forcing of a Simulated Tropical Squall Line**
Imtiaz Dharssi
July 1994

35. **On the nature of the convective circulations at a kata-cold front**
K A Browning
September 1994

36. **Collected preprints of papers submitted to the COST-75 International Seminar on Advanced Weather Radar Systems, Brussels, 20-23 September 1994**
November 1994

37. **Use of satellite imagery to diagnose events leading to frontal thunderstorms: Parts I and II of a case study**
K A Browning and N M Roberts
November 1994

38. **The role of spaceborne millimetre-wave radar in the global monitoring of ice cloud**
P R A Brown, A J Illingworth, A J Heymsfield, G M McFarquhar, K A Browning and M Gosset
December 1994

39. **Potential Vorticity Inversion**
Michal Ziaminaski
October 1994

Met Office Joint Centre for Mesoscale Meteorology Department of Meteorology
University of Reading PO Box 243 Reading RG6 6BB United Kingdom
Tel: +44 (0)118 931 8425 Fax: +44 (0)118 931 8791
www.metoffice.com